

IMECE02/2-6-2-11

IMPORTANCE OF TURBULENCE-RADIATION INTERACTIONS IN TURBULENT REACTING FLOWS

Genong Li

Fluent Incorporated
 10 Cavendish Court
 Lebanon, NH 03766
 Email: gnl@fluent.com

Michael F. Modest

Department of Mechanical Engineering
 The Pennsylvania State University
 University Park, PA 16802
 mfm@mara.me.psu.edu

ABSTRACT

Traditional modeling of radiative transfer in reacting flows has ignored turbulence-radiation interactions (TRI). Radiative fluxes, flux divergences and radiative properties have been based on mean temperature and concentration fields. However, both experimental and theoretical work have suggested that mean radiative quantities may differ significantly from those predictions based on the mean parameters because of their strongly non-linear dependence on the temperature and concentration fields. The composition PDF method is able to consider many nonlinear interactions rigorously, and the method is used here to study turbulence-radiation interactions. This paper tries to answer two basic questions: (1) whether turbulence-radiation interactions are important in turbulent flames or not; (2) if they are important, then what correlations need to be considered in the simulation to capture them. After conducting many flame simulations, it was observed that, on average, TRI effects account for about 1/3 of the total drop in flame peak temperature caused by radiative heat losses. In addition, this study shows that consideration of the temperature self correlation alone is not sufficient to capture TRI, but that the complete absorption coefficient–Planck function correlation must be considered.

NOMENCLATURE

a weight factor in FSK model
 C_ϕ model constant
 C_μ constant in turbulence modeling
 d_j jet diameter

f probability density function
 f_{rad} radiant fraction
 G incident radiation
 ΔH_{comb} heat of combustion
 I radiative intensity
 I_b Planck function
 J_i^α molecular diffusive flux of α -th composition variable
 k spectral dependence part of absorption coefficient
 k turbulent kinetic energy
 L flame length
 \dot{m}_{fuel} mass flow rate of the fuel
 q^R radiative heat flux
 \bar{Q}_{em} radiative emission
 \bar{Q}_{net} net radiative heat loss
 \vec{s} directional vector
 $S_{\text{radiation}}$ source due to radiation
 T temperature
 u spatial dependence part of absorption coefficient
 u_c coflow air velocity
 u_j jet velocity
 u_p pilot flow velocity
 w numerical quadrature weight
 x_i space variable in i th direction
 \underline{Y} species concentration vector
Greek
 κ absorption coefficient
 κ_p Planck mean absorption coefficient
 ρ mixture density
 Ω solid angle

η	wave number
ϕ	composition variables
$\bar{\psi}$	sample space of the composition variables
$\bar{\Gamma}_T$	turbulent diffusivity
ω	turbulent mixing frequency, $= \varepsilon/k$

INTRODUCTION

In turbulent reacting flows the turbulent fluctuations of the flow field cause fluctuations of species concentrations and temperature. Consequently, the radiation field, which is determined by species concentration and temperature fields, will fluctuate as well. In a numerical simulation fluctuations in the radiation field interact with the fluctuations of the flow field, causing the so-called turbulent-radiation interactions (TRI). It has been a great challenge to consider these interactions numerically simulation because they are strongly nonlinear in nature.

For several decades, radiation and turbulence were treated as independent phenomena, and radiative heat fluxes were computed neglecting fluctuations in the radiative intensity and in radiative properties [1]. Some early simple numerical analyses and limited experimental data have indicated the importance of these correlations. Through a Taylor series expansion of the Planck function, Cox [2] estimated that the contribution from temperature fluctuations to radiative emission may dominate the contribution from the mean temperature field when the temperature fluctuation intensity exceeds approximately 40%. Gore et al. [3] showed through experiments that actual radiative fluxes may be two times or more larger than would be expected based on the mean values alone. In the late eighties, some researchers [4–8] performed numerical simulations taking turbulence-radiation interactions (TRI) into account in some simplified fashion, and their predictions were observed to match better with experimental data. In these early studies, either correlations for the turbulent medium or the shape of the PDF had to be assumed. As a result, turbulence-radiation interactions could not be rigorously considered and many claims that were made about TRI need to be further examined.

Probability density function (PDF) methods have the unique feature that many nonlinear interactions can be treated exactly [9], and have been widely used in the modeling of reacting flows in the absence of radiation, in which the chemical reactions, no matter how complicated they are, can be considered exactly [10, 11]. Such methods have been introduced to the study of turbulence-radiation interactions by Mazumder and Modest [12] and by Li and Modest [13]. Mazumder and Modest [12] employed the velocity-composition joint PDF method in their simulation of a bluff body combustor and found inclusion of the absorption coefficient–temperature correlation alone may increase radiative heat flux by 40–45%. The inclusion of velocities and time scale information within the PDF, although allowing closure of more terms, adds further mathematical complexities

to the modeling of the PDF equation as well as stability problem in the numerical simulations. For the purpose of capturing TRI, the composition PDF method is as rigorous as the velocity-composition joint PDF method, but computationally more robust and more efficient. Its use in the study of TRI was demonstrated by Li and Modest [13]. By employing the same method, this paper aims to check the importance of turbulence-radiation interactions, and the relative importance of the different contributions to TRI. Since the Planck function is the most nonlinear function in the radiation calculation, it has been hypothesized that consideration of the temperature self correlation alone can capture most of the TRI [14]. If this were the case, one could treat TRI with the traditional Reynolds average approach, constructing the first few higher moments of temperature. Such issues will be discussed in this paper.

MATHEMATICAL FORMULATION

Turbulence-radiation coupling

In the presence of radiative heat transfer, the energy equation needs to include a radiative source term,

$$S_{\text{radiation}} = -\nabla \cdot \underline{q}^R = \int_0^\infty \kappa_\eta \left(\int_{4\pi} I_\eta d\Omega - 4\pi I_{b\eta} \right) d\eta, \quad (1)$$

where \underline{q}^R denotes the radiative heat flux; κ_η is the spectral absorption coefficient of the radiating gas, which may be a function of temperature T and species concentrations of the radiating medium \underline{Y} ; here I_η is the spectral intensity, $I_{b\eta}$ is the spectral blackbody intensity (or Planck function), the subscript η is used to indicate spectral dependence and Ω denotes solid angle. The radiation intensity is governed by the radiative transfer equation (RTE): for an absorbing-emitting but nonscattering gas, the instantaneous radiant energy balance on a pencil of radiation propagating in direction \vec{s} and confined to a solid angle $d\Omega$ is given by [15],

$$(\vec{s} \cdot \nabla) I_\eta = \kappa_\eta (I_{b\eta} - I_\eta) \quad (2)$$

where the first term on the right-hand side represents augmentation due to emission and the second term is attenuation due to absorption.

To include radiation effects in conventional turbulence calculations, Eqs. (1) and (2) need to be time-averaged, resulting in

$$\langle S \rangle_{\text{radiation}} = \int_0^\infty \left[\int_{4\pi} \langle \kappa_\eta I_\eta \rangle d\Omega - 4\pi \langle \kappa_\eta I_{b\eta} \rangle \right] d\eta, \quad (3)$$

$$\langle \vec{s} \cdot \nabla \rangle I_\eta = \langle \kappa_\eta I_{b\eta} \rangle - \langle \kappa_\eta I_\eta \rangle. \quad (4)$$

Due to the strongly nonlinear dependence of radiative properties on temperature and species concentrations, $\langle \kappa_\eta(T, \underline{Y}) I_\eta \rangle$ does not equal $\kappa_\eta(\langle T \rangle, \langle \underline{Y} \rangle) \langle I_\eta \rangle$ and $\langle \kappa_\eta(T, \underline{Y}) I_{b\eta}(T) \rangle$ does not equal $\kappa_\eta(\langle T \rangle, \langle \underline{Y} \rangle) I_{b\eta}(\langle T \rangle)$, making these two terms unclosed. $\langle \kappa_\eta I_\eta \rangle$ represents a correlation between the spectral absorption coefficient and the spectral incident intensity, and $\langle \kappa_\eta I_{b\eta} \rangle$ represents a correlation between the spectral absorption coefficient and the spectral blackbody intensity. Complete information of the statistics among the composition variables is needed for their determination. For the convenience of later discussion, these two correlations are loosely defined as ‘spectral absorption coefficient–spectral incident intensity correlation’ and ‘spectral absorption coefficient–spectral blackbody intensity correlation’.

The time averaging procedure can be applied to any solution technique for radiation calculation and different unclosed terms may arise for different spectral models and solution methods. However, all of them can be categorized as belonging to two groups: (a) correlations that can be calculated from scalars $\underline{\phi}$ directly or indirectly, and (b) correlations that cannot. The set of scalars $\underline{\phi}$ is defined as

$$\underline{\phi} = (\underline{Y}, T) = (\phi_1, \phi_2, \dots, \phi_s) \quad (5)$$

where s is the total number of scalar variables (number of species plus one) and the last scalar, ϕ_s , is reserved for temperature (or enthalpy). Variables in the set $\underline{\phi}$ are often called the composition variables, since they determine the composition of the mixture.

The unclosed term $\langle \kappa_\eta I_{b\eta} \rangle$ belongs to group (a), since both κ_η and $I_{b\eta}$ are functions of variables in set $\underline{\phi}$ only. The unclosed term $\langle \kappa_\eta I_\eta \rangle$ belongs to group (b), because I_η is not a local quantity, i.e., cannot be expressed in terms of the local scalar variables.

One of the most common approximations made in the open literature on turbulence-radiation interactions is the optically thin eddy approximation as described by Kabashnikov and Myasnikova [16]. Kabashnikov suggested that if the mean free path for radiation is much larger than the turbulence length scale, then the local radiative intensity is weakly correlated with the local absorption coefficient, i.e., $\langle \kappa_\eta I_\eta \rangle = \langle \kappa_\eta \rangle \langle I_\eta \rangle$, in which $\langle \kappa_\eta \rangle$ is loosely defined as the ‘absorption coefficient self correlation.’ The rationale behind these assumptions is that the instantaneous local intensity at a point is formed over a path traversing several turbulent eddies. Therefore, the local intensity is weakly correlated to the local radiative properties. The validity of this assumption depends on the eddy size distribution and the radiation properties of the absorbing gases. In a numerical simulation of combustion chambers, Hartick et al. [8] showed that, although the thin eddy assumption may not be valid over some highly absorbing parts of the spectrum, these spectral zones affect the total radiation exchange only slightly, thus allowing straightforward application of the thin eddy assumption in their simulation. The thin eddy assumption is also employed in the current study. As a result, all

correlations needed to capture TRI belong to group (a).

Radiation Submodel

The radiative transfer equation is a spectrally, spatially and directionally dependent integro-differential equation, and is extremely difficult to solve for general, multi-dimensional geometries. Several approaches are available to reduce this equation to a simpler form. Among them, one of the most popular methods is the P_1 -approximation, in which the incident radiation is governed by a Helmholtz equation, which is relatively easy to solve. For the vast majority of important engineering problems (i.e., in the absence of extreme anisotropy in the intensity field), the method provides high accuracy at very reasonable computational cost. Another challenge in gas radiation calculations comes from the strong spectral dependence of radiation properties. Although line-by-line calculations provide best accuracy, such calculations are too time-consuming for any practical combustion system. Global methods such as the Weighted-Sum-of-Gray-Gases Model (WSGG) are commonly used [17]. Recently, the Full-Spectrum k -Distribution method (FSK) developed by Modest and Zhang [18] has been shown to be superior to the WSGG model, to which it reduces in its crudest implementation. The method is exact within its limitations [gray walls, gray scattering properties, spectral absorption coefficient obeying the so-called scaling approximation, i.e., the spectral and spatial dependence of the absorption coefficient are separable as $\kappa_\eta(\eta, \underline{\phi}) = k_\eta(\eta)u(\underline{\phi})$ where $\underline{\phi}$ are the composition variables]. The P_1 -approximation in conjunction with the FSK model will be used in this study.

Radiative properties and, consequently, the radiative intensity change dramatically across spectral space. In the FSK method the radiative quantities’ spectral dependence has been transformed to a g -dependence, where g is the cumulative distribution function of the absorption coefficient calculated over the whole spectrum and weighted by the Planck function. For example, the source term in the energy equation due to radiative heat transfer is calculated as

$$\begin{aligned} S_{\text{radiation}} &= - \int_0^\infty \kappa_\eta (4\pi I_{b\eta} - G_\eta) d\eta \\ &= - \int_0^1 k_g u (4\pi a_g I_b - G_g) dg \end{aligned} \quad (6)$$

where u is the spatial dependence of the absorption coefficient as mentioned before and a_g is a weight factor introduced during the transformation. The advantage of this transformation lies in the fact that $k_g(g)$ is a smooth, monotonically increasing function of g , thus requiring only a few numerical quadrature points. Readers are referred to [18] for the details about this method. In practical calculations, the integration is replaced by numerical

quadrature. If Gaussian quadrature is used, Eq. (6) becomes

$$S_{\text{radiation}} \approx - \sum_{j=1}^M w_j k_j u (4\pi a_j I_b - G_j), \quad (7)$$

where M is the total number of quadrature points and the w_j are the quadrature weights. The incident radiation G_j must be determined by solving the P_1 -equation, i.e. [15],

$$\nabla \cdot \left(\frac{1}{3k_g u} \nabla G_g \right) = k_g u [G_g - 4\pi a_g I_b] \quad (8)$$

subject to the boundary condition,

$$-\frac{2(2-\epsilon)}{3\epsilon} \hat{n} \cdot \nabla G_g = k_g u (4\pi a_g I_b - G_g) \quad (9)$$

where ϵ is surface emittance and \hat{n} is a unit normal at a boundary surface. The values of $k_g, u(\phi)$ and a_g are obtained from a pre-calculated FSK data base.

Reynolds averaging of the radiative source term and the P_1 -equation leads to

$$\langle S \rangle_{\text{radiation}} = - \sum_{j=1}^M w_j k_j [4\pi \langle u a_j I_b \rangle - \langle u \rangle \langle G_j \rangle] \quad (10)$$

$$\nabla \cdot \left[\frac{1}{3k_j} \frac{1}{\langle u \rangle} \nabla \langle G_j \rangle \right] = k_j \langle u \rangle \langle G_j \rangle - 4\pi k_j \langle u a_j I_b \rangle, \quad j = 1, \dots, M \quad (11)$$

where the optically thin-eddy approximation has been employed. As a result of turbulence-radiation interactions two terms, $k_j \langle u a_j I_b \rangle$ and $k_j \langle u \rangle$, representing correlations between dependent variables, need to be modeled.

Composition PDF Methods

The philosophy of the PDF approach is to treat species concentration and temperature as random variables and consider the transport of their PDFs rather than their finite moments. Once that PDF is known, the mean of any quantity can be evaluated exactly from the PDF, as long as it is a function of the species concentrations or/and temperature. For example,

$$\langle u(\phi) a_j(\phi) I_b(\phi) \rangle = \int u(\underline{\psi}) a_j(\underline{\psi}) I_b(\underline{\psi}) f(\underline{\psi}) d\underline{\psi} \quad (12)$$

$$\langle u(\phi) \rangle = \int u(\underline{\psi}) f(\underline{\psi}) d\underline{\psi} \quad (13)$$

In these equations, $\underline{\psi}$ represents the composition space variable, $\underline{\psi} \equiv (\psi_1, \psi_2, \dots, \psi_s)$, and $f(\underline{\psi})$ is defined to be the probability density of the compound event $\underline{\phi} = \underline{\psi}$ (i.e., $\phi_1 = \psi_1, \phi_2 = \psi_2, \dots, \phi_s = \psi_s$), so that,

$$f(\underline{\psi}) d\underline{\psi} = \text{Probability}(\underline{\psi} \leq \underline{\phi} \leq \underline{\psi} + d\underline{\psi}) \quad (14)$$

In a general turbulent reacting flow, the composition PDF is also a function of space, \underline{x} , and time, t . The transport equation for the composition PDF, $f(\underline{\psi}, \underline{x}, t)$, can be derived from the conservation laws of scalars, which is

$$\begin{aligned} & \frac{\partial}{\partial t} [\rho f] + \frac{\partial}{\partial x_i} [\tilde{u}_i \rho f] + \frac{\partial}{\partial \psi_\alpha} [S_{\alpha, \text{reaction}}(\underline{\psi}) \rho f] \\ & - \sum_{j=1}^M 4\pi w_j k_j \frac{\partial}{\partial \psi_s} [u a_j I_b f] = - \frac{\partial}{\partial x_i} [\langle u_i'' | \underline{\psi} \rangle \rho f] \\ & + \frac{\partial}{\partial \psi_\alpha} \left[\left\langle \frac{1}{\rho} \frac{\partial J_i^\alpha}{\partial x_i} \middle| \underline{\psi} \right\rangle \rho f \right] - \sum_{j=1}^M w_j k_j \frac{\partial}{\partial \psi_s} [u \langle G_j \rangle f] \end{aligned} \quad (15)$$

where i and α are summation indices in physical space and composition space, respectively and $\langle A|B \rangle$ is the conditional probability of the event A , given that the event B occurs.

On the left-hand side of Eq. (15), the first two terms represent the rate of change of the PDF when following the Favre-averaged mean flow. The third term is the divergence of the flux of probability in the composition space due to chemical reaction and radiative emission. The form of this term clearly shows the advantage the PDF method has over moment methods: no matter how complicated and nonlinear these source terms are, they require no modeling. In contrast, the terms on the right-hand side of Eq. (15) need to be modeled. The first two terms represent transport in physical space due to turbulent convection and transport in scalar space due to molecular mixing, respectively. They are usually modeled by using the gradient-diffusion hypothesis and a simple mixing model such as Dopazo's model [9], respectively, leading to

$$-\langle u_i'' | \underline{\psi} \rangle \rho f \approx \Gamma_T \frac{\partial(\rho f)}{\partial x_i}, \quad (16)$$

$$\left\langle \frac{1}{\rho} \frac{\partial J_i^\alpha}{\partial x_i} \middle| \underline{\psi} \right\rangle \approx \frac{1}{2} C_\phi \omega (\psi_\alpha - \bar{\psi}_\alpha) \quad (17)$$

where $\Gamma_T = c_\mu \langle \rho \rangle \sigma_\phi^{-1} k^2 / \epsilon$ is the turbulent diffusivity, and k, ϵ, c_μ and σ_ϕ are, respectively, the turbulent kinetic energy, dissipation rate of turbulent kinetic energy, a modeling coefficient in the standard k - ϵ turbulence model, and turbulent Schmidt or Prandtl numbers; finally, $\omega = \epsilon / k$ is a turbulence 'frequency' and C_ϕ is a

model constant. The third term on the right-hand side of Eq. (15) is closed by invoking the optically thin eddy approximation.

As a result, the modeled transport equation for the composition mass density PDF function is closed and contains all necessary information about all scalars. The composition PDF transport equation is a partial differential equation in $(4 + s)$ dimensions. Traditional finite volume or finite element methods are very inefficient to solve an equation of such high dimensionality. Instead, the Monte Carlo method is generally used, in which the PDF is represented by a large number of computational particles. Each particle evolves in time and space according to a set of stochastic equations and carries with it all composition variables. The PDF is then obtained approximately as a histogram of the particles' properties in sufficiently small neighborhoods in physical space, and the mean quantities are deduced statistically by sampling the particles.

Chemical Reaction Submodel

Although PDF methods allow the use of detailed chemical reaction mechanisms in principle, computational intractability has limited their application. In practice, reduced mechanisms are often used in the PDF calculations. A wide range of reduced mechanisms of chemical reactions for hydrocarbon fuels is available in the literature [19] and the simplest—a single-step skeletal mechanism—is used in this study. It takes the form:



Westbrook and Dryer [20] provided an Arrhenius relationship for the reaction rate of methane as:

$$\frac{d[\text{CH}_4]}{dt} = -A \exp(-E_a/R_u T) [\text{CH}_4]^a [\text{O}_2]^b, \quad (19)$$

where the quantities within square brackets represent molar concentrations; R_u is the universal gas constant, and E_a is the activation energy of the methane. A , a and b are constants in the general Arrhenius equation, which may be obtained from Westbrook and Dryer.

FLAME SIMULATIONS

Flame optical thickness has an important impact on radiative transfer. Three jet flames with different optical thickness have been considered, where flame optical thickness has been defined as

$$\tau = \kappa_P L \quad (20)$$

where κ_P is an average Planck mean absorption coefficient of the participating medium, i.e., the combustion products of H_2O and

CO_2 , and L is the flame length. For turbulent jet flames, flame length is approximately a linear function of jet diameter [21] and, in this study, is estimated to be $L = 40d_j$. The base flame is Sandia's Flame D [22]. The basic experimental setup of this flame is summarized here. The fuel jet ($d_j = 7.2\text{mm}$) with high velocity ($u_j = 49.6\text{m/s}$) is accompanied by an annular pilot flow ($d_p = 18.4\text{mm}$, $u_p = 11.4\text{m/s}$), which is then surrounded by a slow coflow of air ($u_c = 0.9\text{m/s}$). The fuel is a mixture of air and methane with a ratio of 3:1 by volume. A bank of measured data is available for this flame. Detailed information of code validation in the simulation of this flame is reported elsewhere [23] and not repeated in this paper. Flame optical thickness for this flame is 0.237 by Eq. (20). The other two considered (artificial) flames were derived from Flame D by doubling and quadrupling the jet diameter, and their flame optical thickness is 0.474 and 0.948, respectively. For future reference the three flames will be denoted as $\kappa L.1$, $\kappa L.2$ and $\kappa L.3$, respectively.

To simulate these flames, a rectangular axisymmetric computational domain of $70d_j \times 18d_j$ was used, and a non-uniform grid system of 60×70 was found to be fine enough to give grid-independent solutions in the finite volume code. The global time step used in the PDF/particle code was 2.0ms, and 4.0ms and 8.0ms for flames $\kappa L.1$, $\kappa L.2$ and $\kappa L.3$, respectively. For each simulation a total of approximate 1100 iterations was required to get to a statistically stationary result and about 58,000 particles were used in the simulation, taking about 22 cpu hours on a four processor Silicon Graphics O200 machine. The conventional way to define residual error in finite volume methods is meaningless in the hybrid FV/PDF Monte Carlo simulation because the statistical error is generally larger than the truncation error. In the current study, the overall numerical error for a variable ϕ after the j -th iteration is defined as $err = 1/N \sum_{i=1}^N [\phi_i^j - \phi_i^{j-1}]^2 / [\phi_i^{j-1}]^2$, where N is the total number of nodal points. This error never converges to zero, but rather to a value representative of the statistical fluctuation of the solution when steady state is reached. This level mainly depends on the number of particles in the simulation. If temperature is used to monitor the numerical error, a value on the order of 10^{-4} has been reached in the calculations.

Importance of TRI

In order to study turbulence-radiation interactions, three different scenarios were considered for each flame. In the first scenario, radiation is completely ignored in order to study the importance of radiation in flame simulations in general. In the second and third scenarios, radiation is considered but turbulence-radiation interactions are ignored and considered, respectively. The importance of turbulence-radiation interactions can be assessed by comparing numerical results from these two scenarios. By ignoring turbulence-radiation interactions, it is implied that the two unclosed terms $\langle u \rangle$ and $\langle u a I_b \rangle$ are evaluated based on the cell means; when by considering it, these two terms are treated

Table 1. Computed flame peak temperature

Flames	T_{norad} (K)	T_{noTRI} (K)	T_{TRI} (K)	ΔT_{rad} (K)	ΔT_{tri} (K)
$\kappa L.1$	2165	2101	2083	-64	-18
$\kappa L.2$	2161	2016	1952	-145	-64
$\kappa L.3$	2169	1842	1725	-327	-117

exactly.

When comparing numerical results of these three scenarios the most obvious difference is that the flame gets colder and colder as radiation without TRI and radiation with TRI are considered. This is universally true for every flame although the trend is more obvious for flames with large optical thickness. Flame peak temperatures for different flames are tabulated in Table 1. To facilitate the discussion, drops in temperature as a result of considering radiation with/without TRI are also listed in the table. While the peak temperature drops only 64 K and an additional 18 K for a small optical thickness flame, it drops by 145 K and 64 K, respectively, for a medium flame, and by 327 K and 117 K for a large optical thickness flame. While peak temperature applies only to a single point, it usually characterizes the entire temperature field. Figure 1 shows the computed temperature contours for Flame $\kappa L.3$. To examine the differences in more detail, temperature profiles at the axis are shown in Fig. 2. From these figures, it is seen that temperature levels have fallen globally as a result of consideration of radiation and TRI.

From these comparisons, it is clear that radiation cannot just be conveniently ignored in flame simulations, since this would lead to severely overpredicted flame temperatures, which is especially true for large flames, such as Flame $\kappa L.3$. Moreover, turbulence-radiation interactions account for about one third of the total temperature drop due to radiation, and thus turbulence-radiation interactions generally cannot be neglected if radiation is going to be considered in a turbulent flame simulation.

The most important quantity that describes the overall radiation field of a flame is the net radiative heat loss (\dot{Q}_{net}) from the flame, and its normalized variable, the ‘‘radiant fraction’’ (f_{rad}), which is defined as the ratio of the net radiative heat loss to the total heat released during combustion, e.g.,

$$f_{\text{rad}} \equiv \frac{\dot{q}_{\text{rad}}}{\dot{m}_{\text{fuel}} \Delta H_{\text{comb}}} \quad (21)$$

where \dot{m}_{fuel} is the mass flow rate of fuel, and ΔH_{comb} is the heat of combustion. In every simulation, these quantities were calculated and the results are shown in Table 2. As the flame’s optical thickness is increased, the flame radiant fraction increases

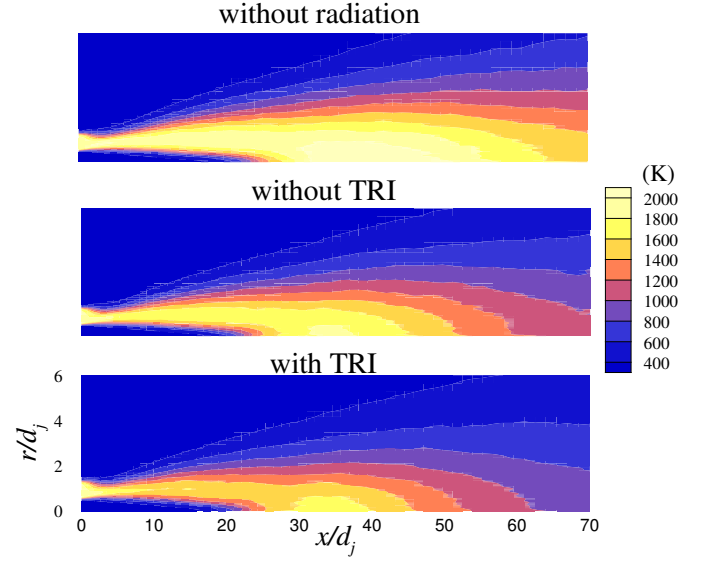


Figure 1. Temperature structure for Flames $\kappa L.3$

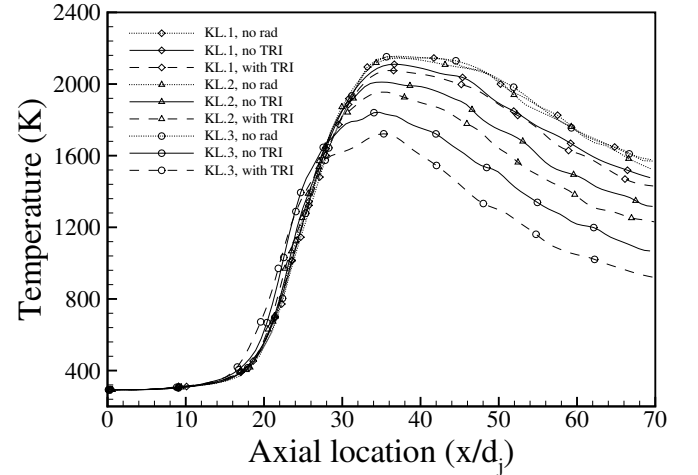


Figure 2. Centerline temperature profiles for Flame κL -series

quickly and the flame gets colder as discussed earlier. In the current study optical thickness was varied by changing the size of the flame. The total potential chemical energy that a fluid particle can release is fixed. Thus, as the flame gets larger, the flow residence time becomes longer, which implies that an average fluid particle will lose more energy through radiation. As a result, the radiant fraction increases as flame size increases. The radiant fraction is only about 5% for Flame $\kappa L.1$, but as high as 18% for Flame $\kappa L.3$. This also explains why temperature levels drop more significantly in optically thick flames. The table also

Table 2. Summary of radiation calculation results

Flame	Without TRI			With TRI			$f^2 - f^1$
	\dot{Q}_{em} (kW)	\dot{Q}_{net} (kW)	f_{rad}^1 (%)	Q_{em} (kW)	\dot{Q}_{net} (kW)	f_{rad}^2 (%)	f^1 (%)
$\kappa L.1$	0.624	0.534	3.05	0.928	0.798	4.56	49
$\kappa L.2$	4.12	2.98	8.51	5.33	3.92	11.2	32
$\kappa L.3$	21.68	12.12	17.3	20.94	12.68	18.1	4.6

shows how the turbulence-radiation interactions enhance radiative heat transfer. For Flame $\kappa L.1$, the net radiative heat loss from that flame is increased from 0.534 kW to 0.798 kW, indicating a 49% increase as a result of turbulence-radiation interactions. In contrast, total radiative heat loss increases by 32% for Flame $\kappa L.2$ and by only 4.6% for Flame $\kappa L.3$ as a result of considering turbulence-radiation interactions. As the flame gets optically thicker, the actual values of radiative heat loss, ignoring TRI and considering TRI, become closer and closer. This does not mean that considering turbulence-radiation interactions is less important for optically thick flames. Radiation calculation is strongly dependent on the flame temperature level and the temperature level has greatly decreased as a result of TRI. Thus, comparison of the radiative loss quantities alone would be misleading.

Importance of Different Correlations

The role of turbulence-radiation interactions on radiative heat transfer can be better understood by isolating their effects on the radiation calculations alone. This can be done by freezing the particle field (including particles' locations, particles' species concentrations and their temperatures) at a point in time, and then calculating radiation fields by ignoring and by considering turbulence-radiation interactions, respectively. Since the same particle field is used, differences in the results of two different simulations are caused entirely by turbulence-radiation interactions. From earlier discussion, it is clear that several terms in the time-averaged governing equations are not closed as a result of turbulence-radiation interactions. The frozen study can also help to differentiate which correlations making up the full TRI are the most important.

From a mathematical point of view, the importance of turbulence-radiation interactions reflects the importance of correlations of $\langle u \rangle$ and $\langle ua_i I_b \rangle$ in the calculations. To illuminate different facets of turbulence-radiation interactions, seven scenarios have been investigated, namely: TRI-N, TRI-1, TRI-2, TRI-3, TRI-4, TRI-5 and TRI-F as summarized in Table 3, where quantities evaluated simply from the mean composition variables are denoted with an overbar. In TRI-N turbulence-radiation interac-

Table 3. Approximations of two TRI terms for different scenarios

Different Scenarios	$k\langle u \rangle$	$k\langle ua_i I_b \rangle$
TRI-N	$k\bar{u}$	$k\bar{u}\bar{a}\bar{I}_b$
TRI-1	$k\langle u \rangle$	$k\bar{u}\bar{a}\bar{I}_b$
TRI-2	$k\langle u \rangle$	$k\langle u \rangle \bar{a}\bar{I}_b$
TRI-3	$k\bar{u}$	$k\bar{u}\bar{a}\langle I_b \rangle$
TRI-4	$k\bar{u}$	$k\bar{u}\langle a I_b \rangle$
TRI-5	$k\bar{u}$	$k\langle ua_i I_b \rangle$
TRI-F	$k\langle u \rangle$	$k\langle ua_i I_b \rangle$

tions are ignored altogether; in TRI-1 only the absorption coefficient self-correlation in the absorption term is considered, with others evaluated at mean property values; in TRI-2 the absorption coefficient self-correlation is considered both in absorption and emission, with the weighted Planck function evaluated at mean property values; in TRI-3 and in TRI-4 the Planck function and the weighted Planck function are considered exactly, respectively (sometimes referred to as "temperature self-correlation"); and in TRI-5, the effects of absorption coefficient-Planck function correlation on emission are also included (but not on absorption); finally, in TRI-F all TRI terms are considered.

The frozen study was performed for every scenario, using particle fields of the fully converged solution for the TRI cases. Table 4 summarizes the results of radiation calculations, including calculated total radiative emission, net radiative heat loss and radiant fraction for each scenario. Comparing results of the cases without TRI and the cases with TRI, the radiant fraction for every flame is increased as a result of considering turbulence-radiation interactions. For example, the radiant fraction is increased by 66%, from 10.9% to 18.1% in Flame $\kappa L.3$. This is in contrast to the results of the coupled flow-radiation calculations (Table 2), in which these quantities are almost identical. Contours of radiative heat loss for this flame are shown in Fig. 3. In most regions, the local radiative heat loss is increased as a result of turbulence-radiation interactions, mainly because the absorption coefficient and the Planck function are positively correlated. The enhancement of radiative heat loss directly depends on the fluctuations of temperature and species concentration fields. These fluctuations are very large at the flame front, and the increase of radiative heat loss is more prominent there, which can be observed more clearly from their profiles at one cross-section and at the centerline as shown in Fig. 4.

Effects of $\langle u \rangle$

The absorption coefficient self correlation, $k_i\langle u \rangle$, appears in the absorption term of Eq. (10), i.e., $\sum w_i k_i\langle u \rangle \langle G_i \rangle$. Comparing the TRI-N case and the TRI-1 case, the only difference is that

Table 4. Comparison of radiation calculation results for series of κL -flames

Flame	Scenarios	\dot{Q}_{em} (kW)	\dot{Q}_{net} (kW)	f_{rad} (%)
Flame $\kappa L.1$	TRI-N	0.597	0.516	2.94
	TRI-1	0.597	0.507	2.90
	TRI-2	0.657	0.558	3.19
	TRI-3	0.812	0.706	4.03
	TRI-4	0.641	0.555	3.17
	TRI-5	0.928	0.820	4.68
	TRI-F	0.928	0.798	4.56
Flame $\kappa L.2$	TRI-N	3.42	2.51	7.14
	TRI-1	3.42	2.45	6.98
	TRI-2	3.73	2.68	7.64
	TRI-3	4.59	3.42	9.74
	TRI-4	3.69	2.73	7.78
	TRI-5	5.33	4.02	11.5
	TRI-F	5.33	3.92	11.2
Flame $\kappa L.3$	TRI-N	12.7	7.63	10.9
	TRI-1	12.7	7.44	10.6
	TRI-2	13.8	8.03	11.5
	TRI-3	17.5	10.67	15.1
	TRI-4	14.2	8.63	12.3
	TRI-5	20.9	13.1	18.7
	TRI-F	20.9	12.7	18.1

the absorption coefficient self-correlation is considered in the absorption term for the TRI-1 case. The computational results in Table 4 show that flame absorption is increased as a result of considering this correlation. This is true for every flame. But the magnitude of change is quite small, e.g., 10% for Flame $\kappa L.1$, 7% for Flame $\kappa L.2$ and 4% for Flame $\kappa L.3$, indicating that the exact consideration of this correlation is not very important. This is expected, since the absorption coefficient is linearly dependent on species concentrations and almost linearly dependent on temperature, so that $\langle u \rangle$ is close to \bar{u} . This also explains why TRI-1 and TRI-2, and TRI-5 and TRI-F, respectively, lead to similar results.

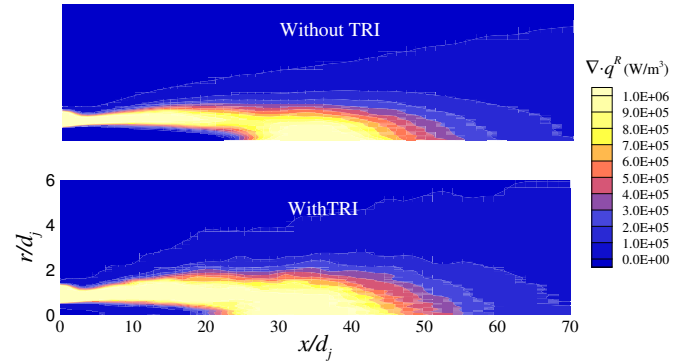


Figure 3. Contours of radiative heat loss from Flame $\kappa L.3$

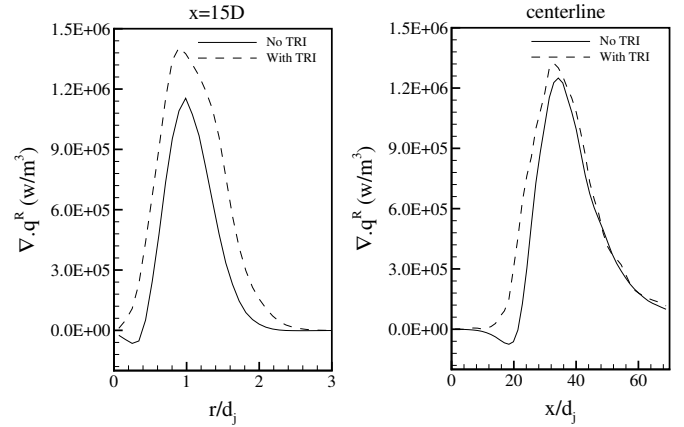


Figure 4. Profiles of radiative heat loss at one cross-section and at the centerline for Flame $\kappa L.3$

Effects of $\langle ua_j I_b \rangle$

The absorption coefficient-Planck function correlation, $\langle ua_j I_b \rangle$, appears in the emission term of Eq. (10), i.e., $\sum 4\pi w_i k_i \langle ua_j I_b \rangle$. In the TRI-5 case, only this correlation is considered in the calculations. Comparing the numerical results of this case with those of the TRI-N case, flame emission, absorption and total net heat loss all have increased dramatically, e.g., radiative heat loss has increased by 59% in Flame $\kappa L.1$, 60% in Flame $\kappa L.2$ and 72% in Flame $\kappa L.3$, indicating the importance of this correlation.

The Planck function is the most nonlinear function in the absorption coefficient-Planck function correlation. It has been suggested that consideration of the Planck function self-correlation (or temperature self correlation) alone may be enough to cap-

ture the essence of turbulence-radiation interactions. If this were true, only temperature fluctuations would be required to capture turbulence-radiation interactions, since the Planck function depends only on temperature; fluctuations of species concentrations would have no impact, which would greatly simplify the analysis of turbulence-radiation interactions. TRI-3 and TRI-4 cases were designed specifically to answer this question. Comparing the results of TRI-N and TRI-3, the total radiative heat loss is increased about 37%, 36% and 39%, respectively, for each case as a result of considering the Planck function. For non-gray gases, the weighted Planck function should be used in calculation of the temperature self correlation. Comparing results of TRI-3 with those of TRI-4, it is interesting to see that the consideration of $\langle aI_b \rangle$ considerably diminishes the total radiative heat loss. This indicates that turbulence-radiation effects may have less important impact in strongly non-gray media than in gray media. Even for a gray case, the Planck function self-correlation accounts for about 60% of total TRI; therefore, considering only this correlation would be insufficient. It is also interesting to note that, although the absorption coefficient self-correlation and the weighted Planck function self correlation are not important, the positive correlation between them makes the absorption coefficient-Planck function correlation very important.

CONCLUSIONS

The composition PDF method was used to study radiating reactive turbulent flows. The method is able to treat turbulence-radiation interactions in a rigorous way: many unclosed terms due to TRI in the conventional moment method can be calculated exactly. Effects of turbulence-radiation interactions were investigated by comparing two different simulations of several 2D jet flames: one ignores turbulence-radiation interactions and the other considers them. The simulations show that, by ignoring TRI, radiation heat losses are always severely underpredicted and, consequently, temperature levels are generally substantially overpredicted. In addition, through freezing species concentrations and temperature fields, the importance of different TRI-related correlations were investigated. Numerical results show that, in order to determine turbulence-radiation interactions, consideration of the temperature-self correlation alone is not sufficient (although non-linearity of the Planck function with temperature is the severest among other functions), the absorption coefficient-Planck function correlation must also be considered.

ACKNOWLEDGMENTS

The authors are grateful to the National Science Foundation for funding of this research under grant number CTS-9732223.

REFERENCES

- [1] Viskanta, R. and Menguc, M. P., 1987, "Radiation Heat Transfer in Combustion Systems", *Progress in Energy Combustion Science*, **13**, pp. 97–160.
- [2] Cox, G., 1977, "On Radiant Heat Transfer from Turbulent Flames", *Combustion Science and Technology*, **17**, pp. 75–78.
- [3] Faeth, G. M., Gore, J. P., Shuech, S. G., and Jeng, S. M., 1989, "Radiation from Turbulent Diffusion Flames", *Ann. Rev. Numer. Fluid Mech. Heat Trans.*, **2**, pp. 1–38.
- [4] Song, T. H. and Viskanta, R., 1987, "Interaction of Radiation with Turbulence: Application to a Combustion System", *J. Thermophysics*, **1**(1), pp. 56–62.
- [5] Soufiani, A., Mignon, P., and Taine, J., 1990, "Radiation Effects on Turbulent Heat Transfer in Channel Flows of Infrared Active Gases", *Radiation Heat Transfer: Fundamentals and Applications*, *HTD*, **137**, pp. 141–148.
- [6] Soufiani, A., Mignon, P., and Taine, J., 1990, "Radiation-Turbulence Interaction in Channel Flows of Infrared Active gases", *Proceedings of International Heat Transfer Conference*, **6**, pp. 403–408.
- [7] Hall, R. J. and Vranos, A., 1994, "Efficient Calculations of Gas Radiation from Turbulent Flames", *Int. J. Heat Mass Transfer*, **37**(17), pp. 2745–2750.
- [8] Hartick, J. W., M., Tacke, Fruchtel, G., Hassel, E. P., and J., Janicka, 1996, "Interaction of Turbulence and Radiation in Confined Diffusion Flames", *Twenty-Sixth Symposium (International) on Combustion*, **26**, pp. 75–82.
- [9] Pope, S. B., 1985, "PDF Methods for Turbulent Reactive Flows", *Progress in Energy and Combustion Science*, **11**, pp. 119–192.
- [10] Kollmann, W., 1990, "The PDF Approach to Turbulent Flow", *Theor. Compt. Fluid Dyn.*, **1**, pp. 249–285.
- [11] Dopazo, C., 1994, "Recent Developments in PDF Methods", In Libby, P. A. and William, F. A., eds., *Turbulent Reacting Flow*, Academic Press, San Diego, pp. 375–474.
- [12] Mazumder, S. and Modest, M. F., 1998, "A PDF Approach to Modeling Turbulence-Radiation Interactions in Nonluminous Flames", *International Journal of Heat and Mass Transfer*, **42**, pp. 971–991.
- [13] Li, G. and Modest, M. F., 2002, "Application of Composition PDF Methods in the Investigation of Turbulence-radiation Interactions", *Journal of Quantitative Spectroscopy & Radiative Transfer*, **73**, pp. 461–472.
- [14] Burns, S. P., 1999, "Turbulence Radiation Interaction Modeling in Hydrocarbon Pool Fire Simulation", *SAND 99-3190*.
- [15] Modest, M. F., 1993, *Radiative Heat Transfer*, McGraw-Hill, New York.
- [16] Kabashnikov, V. P. and Myasnikova, G. I., 1985, "Thermal Radiation in Turbulent Flows-Temperature and Concentration Fluctuations", *Heat Transfer-Soviet Research*, **17**(6),

pp. 116–125.

- [17] Hottel, H. C. and Sarofim, A. F., 1967, *Radiative Transfer*, McGraw-Hill, New York.
- [18] Modest, M. F. and Zhang, H., 2002, “The Full-Spectrum Correlated- k Distribution For Thermal Radiation from Molecular Gas–Particulate Mixtures”, *ASME Journal of Heat Transfer*, **124**(1), pp. 30–38.
- [19] Dryer, F. L. and Glassman, I., 1972, “High-temperature Oxidation of CO and CH₄”, *Fourteenth Symposium (International) on Combustion*, pp. 987–1003.
- [20] Westbrook, C. K. and Dryer, F. L., 1981, “Simplified Reaction Mechanisms for the Oxidation of Hydrocarbon Fuels in Flames,” *Combustion Science and Technology* , **27**, pp. 31–43.
- [21] Turns, S. R., 2000, *An Introduction to Combustion: Concepts and Applications*, McGraw-Hill, Boston.
- [22] Barlow, R. S. and Frank, J. H., 1998, “Effects of Turbulence on Species Mass Fractions in Methane/Air Jet Flames”, *Proceedings of the Twenty-Seventh Symposium (international) on Combustion*, pp. 1087–1095.
- [23] Li, G. and Modest, M. F., 2002, “Investigation of Turbulence-radiation Interactions in Turbulent Jet Flames”, *in preparation*.